IOSR Journal of Mechanical and Civil Engineering (IOSR-JMCE)
e-ISSN: 2278-1684,p-ISSN: 2320-334X, Volume 17, Issue 1 Ser. II (Jan - Feb 2020), PP 48-60
www.iosrjournals.org

Thermal Analysis of Melting Process with Conjugate Turbulent Flow Convection of Liquid Metal Fluid in Mini-scaled Thermal Storage Channel

M Khamis Mansour[1, 2,] M.K. Elyoussef[1]
[1]*Department of Mechanical Engineering, Faculty of Engineering, Beirut Arab University*
[2]*Department of Mechanical Engineering, Faculty of Engineering, Alexandria University*

Abstract: *This article presents thermal modeling of conjugate heat transfer problem of liquid metal fluid in mini-scaled thermal storage. The heat transfer conjugate problem consists of turbulent convective flow of the heat transfer fluid (HTF) and melting process in the phase change material (PCM). The Sodium-Potassium (NaK) liquid metal fluid was selected as the HTF while the paraffin wax was used as the PCM. The local Nusselt (Nu) number represents the thermal behavior of the HTF; alternatively, the melting heat characteristics was reported by the average liquid fraction of the PCM. The present model was verified by comparison its results to those obtained from previous work in the literature. There was a decent concord between both results with maximum deviation of 10 %. A parametric study has been accomplished to show the influence of operational and geometrical design factors on the thermal behavior of the conjugate problem. The length to diameter ratio (L/D) represents the geometrical parameter. However, Reynolds (Re) number, Stefan (Ste) number, and Fourier (Fo) number represents the operational parameters. The parametric study has been carried out during presence/absence of the free convection of the PCM through the melting process. It was found from the parametric study that the (L/D), Ste, and Fo have no impact on the local Nu number at fully developed region except the Re number. On the other hand, sometimes the minichannel which is featured by the absence of natural convection can be superior that during the occurrence of free convection at variation of some parameters. The result obtained from the parametric study showed that the fully-developed Nu number approaches that of traditional standard correlation of constant wall temperature (CWT) problem.*
Keywords: *Melting process, conjugate problem, forced convection, natural convection, mini-channel thermal storage*

Date of Submission: 15-01-2020 Date of Acceptance: 03-02-2020

List of Symbols

d_o	Outer mini-channel tube diameter, m
d_i	Inner mini-channel tube diameter, m
L	Length of the mini-channel, m
K	Thermal conductivity, W/(m.^{o}K)
Nu	Local Nusselt number
P	Pressure, Pa (gauge value)
Re	Reynolds number
Ste	Stefan number
Fo	Fourier number
L/D	Length to diameter of the mini-channel
x, y, z	Cartesian coordinates
T	Temperature, ^{o}K
Y	Incremental length of the unit cell, m
Y^*	Non-dimensionnel thermal axial length, Y/L
T_{in}	Inlet fluid temperature, ^{o}K
T_{HTF}	fluid temperature, ^{o}K
T_{PCM}	Phase change material temperature, ^{o}K
V	Inlet fluid velocity, m/sec

Greek Symbols

γ Liquid Fraction

Subscripts

in inlet
t Time
f Heat transfer fluid

Abbreviations

MC Mini-channel
HTF Heat transfer fluid
PCM Phase change materials
WNC With natural convection
WONC Without natural convection
CHF Constant heat flux
CHT Coefficient of heat transfer
CWT Constant wall temperature

I. Introduction

Nowadays, carbon dioxide emissions and other harmful gases are spreading widely, which may be a challenge in order to overcome this issue by showing and using another sources then oil energies, for this reason renewable energies are highly considered as a good sources aiming to take the role of petroleum sources. Thermal energy storage systems are used in many renewable energy applications in which these systems are prime important nowadays presenting in several domains such as construction, manufacturing and electricity generation [1]. This makes the thermal energy storage system important in several engineering applications as using in heating and cooling systems. The latent heat storage is widely used in industry to high value of stored energy per unit volume [2]. On the other hand, recently there has been a fast development in the mini/micro scale heat exchanger technology. This new technology motivates many researchers to investigate the thermal characteristics of those heat exchangers. This study mainly focuses on mini-scaled thermal storage channel design and its thermal behavior. The mini-channel (MC) consists of a PCM imbedded inside its outer tube where a HTF flows inside the inner tube of this channel. The PCM absorbs the thermal energy released from the HTF and stores it as a latent heat capacity and cooling the HTF, this leads to have a conjugate problem associates the melting process of the PCM as well as the single-phase fluid flowing inside the MC (see Figure 1). The vertical position of the minichannel causes an occurrence of the free convection currents during the melting process. Therefore, all of these aspects make the heat transfer problem to be complicated to some extent and gives some interests to be studied and investigated.

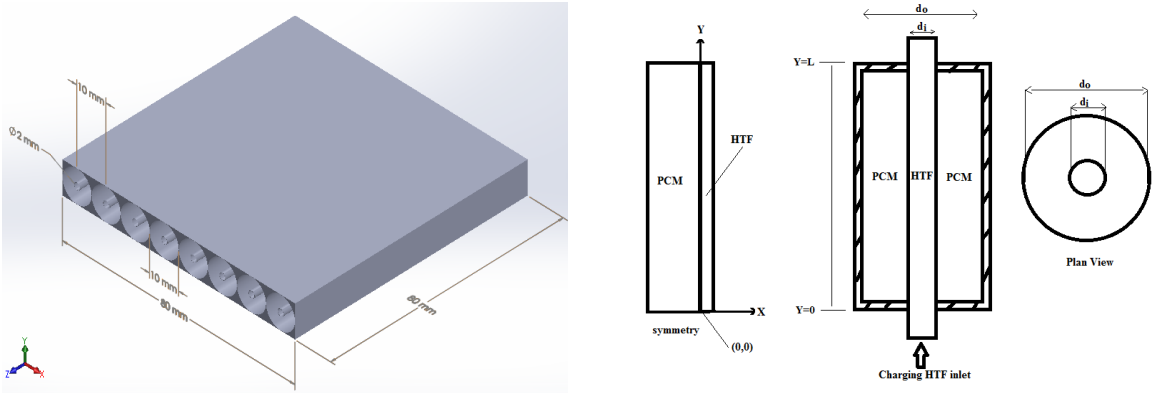

Figure 1. 3D and 2D view of the presented MC model

A melting process during the presence of natural convection has been investigated by many researchers, all of those researchers analyzed the effect of natural convection on the melting process itself either theoretically (numerically or analytically) or experimentally or both [3]. They concluded that the natural convection currents improve the melting process by shorting the time required for the melting process.

However, most of the previous research works focused only on the melting process during the presence of the natural convection without attention to the heat characteristics of the HTF, or to solving the conjugate heat transfer coupling between the HTF and PCM [3].

According to the available literature, a few studies treated the conjugate heat transfer problem during the melting process. Some of the research works [4-11] addressed the HTF flow inside the conduit as fully developed and adopted ordinary equations to determine the convective heat transfer coefficient (HTC) of the HTF for CWT and constant heat flux (CHF) boundary conditions. Other researchers [12-15] solved the momentum and energy equations for the HTF with neglecting of free convection experienced in the melted PCM liquid.

Zhang and Faghri [16] studied a hollow cylinder containing PCM with HTF pumped in the interior of the cylinder by semi-analytical method forming a conjugate problem. Nu number was studied along the cylinder with different lengths. The results showed that the convection inside the tube never reached the fully developed state either with maximum tube length (L/D > 100), this leads to realize that the laminar forced convective heat transfer for HTF of moderate Prandtl number (water) must be solved as a conjugate problem with the PCM [16]. The results were achieved during absence of free convection mode. Cao and Faghri [17] have numerically studied a thermal storage system. They concluded that the phase change for PCM and the unsteady forced convection heat transfer for HTF with low Prandtl number must be treated as conjugate melting problem [17]. The study was carried out during absence of natural convection. Also, they carried out an optimization process for different L/D ratios. Recently, M Khamis Mansour [3] simulated numerically and experimentally 3-D conjugate heat transfer problem in MC. The paraffin wax was used as a PCM while the water was used as a HTF. Experimental work has been done to validate the numerical results. The effect of inlet temperature and velocity of the HTF were taken into account. Results showed that natural convection during the PCM melting shortens the fusion time and makes the wax at the outlet face of the MC to melt faster than that at the inlet face [3]. The results also showed that the local Nu number trends in the conjugate heat transfer problem during melting at the presence of natural convection are different compared to the traditional trends at CHF and CWT as boundary conditions [3].

It can be concluded from pervious paragraphs that the study of the conjugate problem in the melting process is very scare, particularly at with natural convection (WNC) currents. In addition, the effect of the geometrical and the operational variables at the conjugate problem thermal characteristics are not extensively addressed yet according to the author's knowledge. The main objective of this study is to conduct a parametric study for the effect of the key design parameters on the conjugate heat transfer problem during the melting problem and to determine the Nu number correlation of the convective HTC of the HTF.

II. Mathematical Model

Again, the conjugate heat transfer problem consists of co-axial tubes where the HTF flows inside the inner tube of diameter (d_i) and the PCM bounds the outer tube of diameter (d_o). A particular cell is chosen as a yardstick in order to imitate the conjugate problem of the MC as well as to solve the problem in 2D forms [3]. This is accredited to the symmetrical shape of the various cells making the MC. The model geometry is presented in Figure 1.

2.1 Model assumptions

The 2D flow is studied using commercial software ANSYS FLUENT 14.5 under transient condition with the following assumptions:

- Turbulent and incompressible
- Constant thermo-physical properties
- The liquid phase's density varies linearly with the temperature as in the Boussinesq approximation [3].
- Viscous heat dissipation is neglected [3]
- Natural convection is incompressible, Newtonian, and laminar flow [3]
- Density difference between the liquid phase and solid phase of the PCM is negligible [3]
- Radiation heat is neglected
- No heat generation

2.2 Governing equations

HTF domain

Continuity equation

The continuity equation is:

$$\frac{\partial \rho}{\partial t} + \rho\left(\frac{\partial V_x}{\partial x} + \frac{\partial V_y}{\partial y}\right) = 0 \quad (1)$$

Momentum equation

The momentum conservation is given by:

$$\rho\left(\frac{\partial V_x}{\partial t} + V_x\frac{\partial V_x}{\partial x} + V_y\frac{\partial V_x}{\partial y}\right) = -\frac{\partial P}{\partial x} + \mu\left[\frac{\partial^2 V_x}{\partial x^2} + \frac{\partial^2 V_x}{\partial y^2}\right] + \rho g_x \quad (2)$$

$$\rho\left(\frac{\partial V_y}{\partial t} + V_x\frac{\partial V_y}{\partial x} + V_y\frac{\partial V_y}{\partial y}\right) = -\frac{\partial P}{\partial y} + \mu\left[\frac{\partial^2 V_y}{\partial x^2} + \frac{\partial^2 V_y}{\partial y^2}\right] + \rho g_y \quad (3)$$

Energy equation

The energy equation is:

$$\rho_f C_p\left(\frac{\partial T_f}{\partial t} + V_x\frac{\partial T_f}{\partial x} + V_y\frac{\partial T_f}{\partial y}\right) = K_f\left(\frac{\partial^2 T_f}{\partial x^2} + \frac{\partial^2 T_f}{\partial y^2}\right) \quad (4)$$

Where ρ is the density, V is the velocity component, p is the pressure, μ is the dynamic viscosity, P is the pressure, g is the gravity, Cp is the specific heat, K_f is fluid thermal conductivity, T_f is the fluid temperature and x and y are the 2-D Cartesian coordinates.

The k-epsilon model was employed to determine the turbulent flow of the HTF.

$$\frac{\partial(\rho k)}{\partial t} + \frac{\partial(\rho k u_i)}{\partial x_i} = \frac{\partial}{\partial x_j}\left[\frac{\mu_t}{\sigma_k}\frac{\partial k}{\partial x_j}\right] + 2\mu_t E_{ij}E_{ij} - \rho\grave{o} \quad (5)$$

$$\frac{\partial(\rho\grave{o})}{\partial t} + \frac{\partial(\rho\grave{o}u_i)}{\partial x_i} = \frac{\partial}{\partial x_j}\left[\frac{\mu_t}{\sigma_{\grave{o}}}\frac{\partial\grave{o}}{\partial x_j}\right] + C_{1\grave{o}}\frac{\grave{o}}{k}2\mu_t E_{ij}E_{ij} - C_{2\grave{o}}\rho\frac{\grave{o}^2}{k} \quad (6)$$

Where K is the turbulence kinetic energy while Ɛ represents the turbulence dissipation.

PCM domain

In the PCM domain, enthalpy-porosity technique was used to stimulate the model in ANSYS FLUENT during solidification/melting process. The melt interface is not tracked explicitly by this technique. Instead, a quantity called the liquid fraction, which indicates the fraction of the cell volume that is in liquid form, is associated with each cell in the domain [3]. The liquid fraction is computed during each iteration, based on an enthalpy balance. The mushy zone is a region in which the liquid fraction lies between 0 and 1 [3]. The mushy zone is modeled as a porous medium in which the porosity decreases from 1 to 0 as the material solidifies [3]. When the material has fully solidified in a cell, the porosity becomes zero and hence the velocities also drop to zero [3]. The equations are the following, given in Cartesian co-ordinates as follows:

Continuity equation

The continuity equation is:

$$\frac{\partial}{\partial x_i}\left(\rho V_i\right) = 0 \quad (7)$$

Momentum equation

The momentum conservation is:

$$\frac{\partial}{\partial t}\left(\rho V_j\right) + \frac{\partial}{\partial x_i}\left(\rho V_i V_j\right) = \mu\frac{\partial^2 V_j}{\partial {x_i}^2} - \frac{\partial P}{\partial x_j} + \rho g_j + Si \quad (8)$$

Energy equation

The energy equation is:

$$\frac{\partial}{\partial t}(\rho H)+\frac{\partial}{\partial x_i}(\rho V_i H)=\frac{\partial}{\partial x_i}\left(k\frac{\partial T}{\partial x_i}\right) \quad (9)$$

As in M Khamis Mansour [3], ρ is the density, k is the thermal conductivity, μ is the dynamic viscosity, P is the pressure, Si is the momentum source term, V is the velocity component, x is the Cartesian coordinate, and H is the enthalpy of the material is computed as the sum of the sensible enthalpy, h, and the latent heat, ΔH:

$$H = h + \Delta H \quad (10)$$

Where, $h = h_{ref} + \int_{Tref}^{T} C_p dT$ and $\Delta H = \gamma L_f$

h_{ref} is the reference enthalpy at the reference temperature T_{ref}, C_p is the specific heat, L_f is the latent heat, and γ is the liquid fraction during the phase change which occurs over a range of temperatures $T_s < T < T_l$ defined by the following relations:

$$\gamma = \frac{\Delta H}{L_f} = 0 \quad \text{if} \quad T_s < T \qquad \text{[Solid]} \quad (11)$$

$$\gamma = \frac{\Delta H}{L_f} = \frac{T - T_s}{T_l - T_s} \quad \text{if} \quad T_s < T < T_l \qquad \text{[Mushy]} \quad (12)$$

$$\gamma = \frac{\Delta H}{L_f} = 1 \quad \text{if} \quad T > T_l \qquad \text{[Liquid]} \quad (13)$$

The source term S_i in the momentum equation is given by:

$$S_i = -A(\gamma)V_i = \frac{C(1-\gamma)^2}{\gamma^3 + \varepsilon}V_i \quad (14)$$

Where $A(\gamma)$ is defined as the "porosity function" which reduces the velocities gradually from a finite value as 1 in fully liquid to 0 in fully solid state within the computational cells involving phase change. ε is a small number (0.001) to prevent division by zero and C is the mushy zone constant, it measures the amplitude of the damping; the higher this value, the steeper the transition of the velocity of the material to zero as it solidifies [3].

2.3 Boundary Conditions

Inlet section

At the inlet section for the HTF domain, the velocity and temperature are considered as uniform while for the PCM the velocity is zero and the walls are adiabatic.

$$\text{At y = 0, } 0 \le x \prec \frac{d_i}{2} \text{ , at } t \ge 0 \qquad V_x = 0, V_y = V_{in}, T_f = T_{in} \quad (15)$$

Outlet section

If in ANSYS FLUENT, the details of the flow velocity and pressure are not known prior to the solution of the flow problems, the outlet boundary conditions are used to model flow exits. At the outflow boundary conditions, it is first assumed a zero normal gradient for all the variables except pressure. Then, ANSYS FLUENT updates those gradients in the model calculations [3].

$$\text{At y = L, } 0 \le x \prec \frac{d_i}{2} \text{, at } t \ge 0 \quad \frac{\partial V_x}{\partial y} = \frac{\partial V_y}{\partial y} =, \frac{\partial T}{\partial y} = 0 \quad (16)$$

Walls

Walls surrounded the PCM are assumed adiabatic except the interface wall between the PCM and HTF.

$$\frac{d_i}{2} \le x \le \frac{(d_o - d_i)}{2}, \text{y = 0, at } t \ge 0 \qquad \frac{\partial T_s}{\partial y} = 0, V_x = V_y = 0 \qquad (17)$$

$$\frac{d_i}{2} \le x \le \frac{d_o - d_i}{2}, \quad \text{y = L, at } t \ge 0 \qquad \frac{\partial T_s}{\partial y} = 0, V_x = V_y = 0 \qquad (18)$$

$$x = \frac{d_o}{2}, 0 \le y \le L, \text{ at } t \ge 0 \qquad \frac{\partial T_s}{\partial x} = 0, V_x = V_y = 0 \qquad (19)$$

$$\text{at x = 0, } 0 \le y \prec L \text{ , at } t \ge 0 \qquad V_x = \frac{\partial V_y}{\partial x} = \frac{\partial T}{\partial x} = 0 \quad \text{(symmetry)} \qquad (20)$$

$$\text{At } 0 \prec y \prec L, \; x = \frac{d_i}{2}, \text{at } t \ge 0$$

$$V_x = V_y = 0, (K_{PCM} \frac{\partial T}{\partial y})_{PCM} = (K_{HTF} \frac{\partial T}{\partial y})_{HTF}, \text{and } T_{PCM} = T_{HTF}$$

At PCM – HTF interface, no-slipping condition is assumed and no heat generation or thermal contact resistance does not exist.

Initial conditions

The initial temperatures of the HTF is T_{in} and PCM is 300°K.

III. Model Validation

In this part, the numerical results gotten from the present model are verified via the evaluation with results found in Cao and Faghri [17] with low Prandtl number fluid of 0.004 was used as the HTF. Figure 2 is prepared to show the assessment between the results of two models at specific conditions listed in this Figure. There is a decent conformity between both results with maximum discrepancy of to 1.33% occurs at X =7.5 as shown in Figure 2

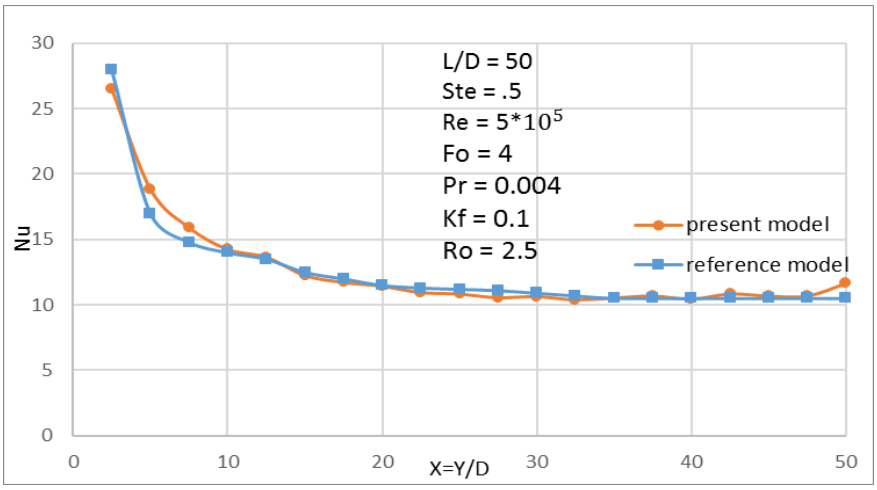

Figure 2. Nu number along the MC length at Fo=4; calculated and from Zhang and Faghri [5]

IV. Results and Discussion

This section is separated into two parts; the first one discusses the impact of the operational and geometrical and input variables on the conjugate problem's thermal characteristics. The length-to-diameter ratio (L/D), Reynolds (Re) number, Stefan (Ste) number, and Fourier (Fo) number are employed as the key design parameters. The local Nu number for the HTF and average liquid fraction (γ) for the PCM represent the thermal

characteristics of the conjugate heat transfer problem. The second part of this section focuses on developing the new correlations for the calculations of average Nu number and its validation and comparison with predictions via the traditional correlations in the references (constant wall temperature (CWT) and constant heat flux (CHF)).

4.1 Parametric study

4.1.1 Effect of L/D ratio

The results of the effect of the key parameters are presented into two categories, the first one is at high Re number of 1500 (high mass flow rate) and the second one is at low Re number (low mass flow rate). In addition, there is a difference between the trend of the local Nu number in case of presence of natural convection (PNC) and that at absence of natural convection (ANC) currents. As noticed in Figure 3a, the trend of the local Nu number in case of PNC surfers from a steep decline at the end of the channel. The explanation of that is at the end of the channel, the free convection currents accommodate and make this zone to be hot. This hot zone decreases the magnitude of the heat flux at it, as displayed in Figure 3b, and accordingly the local Nu number decreases. The effect of the key parameters will be studied on the minichannel during PNC, therefore, all the following graphs of local Nu number will be ended by steep decline as noticed in Figure 3a.

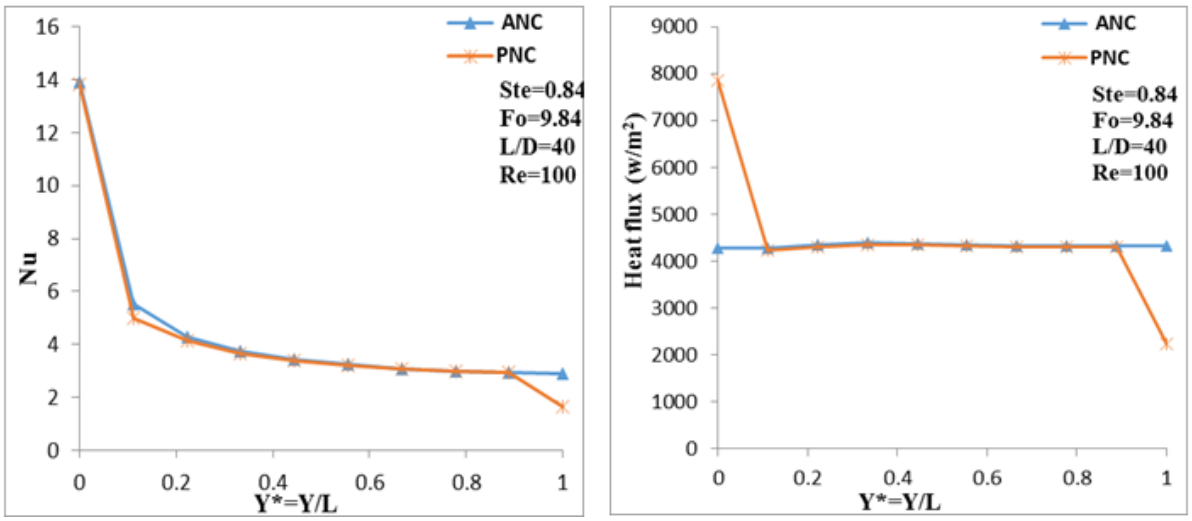

Figure 3. Comparison between MC thermal characteristics during PNC and ANC
a)- Local Nu number b)-Wall heat flux

As shown in Figures 4a and 4b, the decrease in L/D ratio accounts to an increase in Nu number and this conforms to what be expected of the output of Sieder-Tate [17] traditional correlation for the thermal entrance region. In addition, the change in L/D ratio has a noticeable difference on the local Nu number in case of high mass flow rate of HTF (high Re) compared to that at low Re number. This can be explained by that at small Re number the entrance length is very short, therefore, the increase in L/D at low Re number makes the channel approaches the thermal developed zone. In turn, the difference in Nu number in the thermal developed zone is insignificant; therefore, the increase or decrease in L/D has trivial effect on the Nu number at low Re as confirmed by Figure 4b.

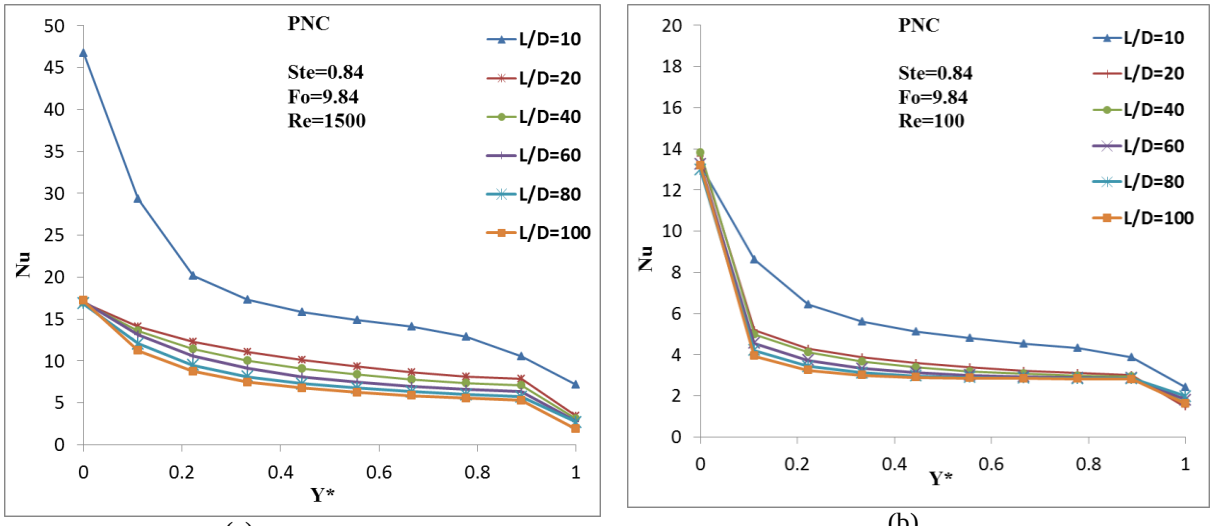

(a) (b)

Figure 4. Impact of L/D ratios on Local Nu number: (a) Re=1500, (b) Re=100

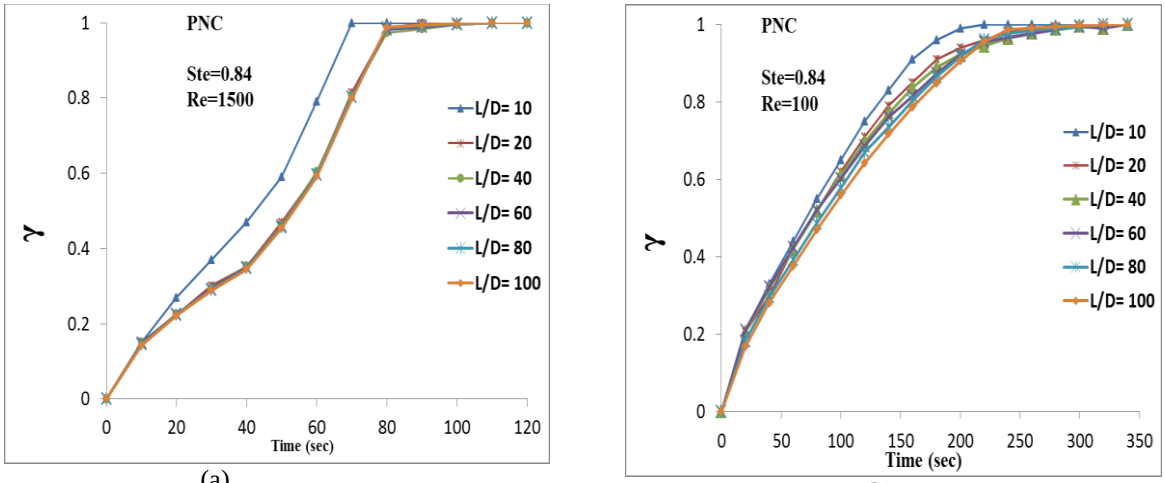

(a) (b)

Figure 5. Impact of L/D ratios on average liquid fraction: (a) Re=1500, (b) Re=100

On the other hand, it is interesting to observe that although the change in L/D ratio has a noticeable difference on the local Nu number at high Re number, however, it has no effect on the average liquid fraction (particularly for L/D >= 20) as depicted in Figure 5a. This is attributed to that at high mass flow rate of the HTF the inner HTC is high, this causes the wall temperature (at the interface) approaches the HTF temperature, which is almost constant due to high flow rate. Hence, the wall temperature is almost constant with changing in L/D ratio. The wall temperature is the responsible of generating the natural convection currents, which assists the melting process. Accordingly, there is no effect on the melting rate at different L/D ratio at high Re number.

It can be summarized that the mini-channel designer has no need to select longer channel (high L/D ratio) because this does not accredit the melting rate process and the need for longer channel is considered only when the designer targets large thermal stored energy (large mass of the wax). However, at low Re number (low inlet velocity), the longer channel causes lengthy melting time as shown in Figure 5b.

4.1.2 Effect of Stefan (Ste) number

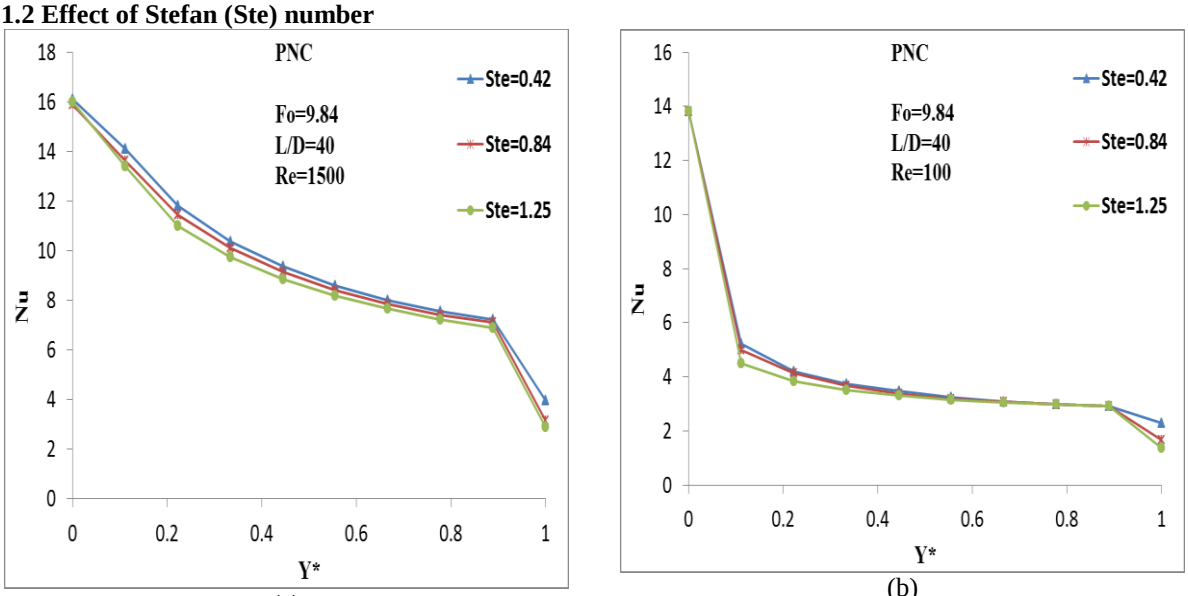

(a) (b)

Figure 6. Impact of Ste number on Local Nu number: (a) Re=1500, (b) Re=100

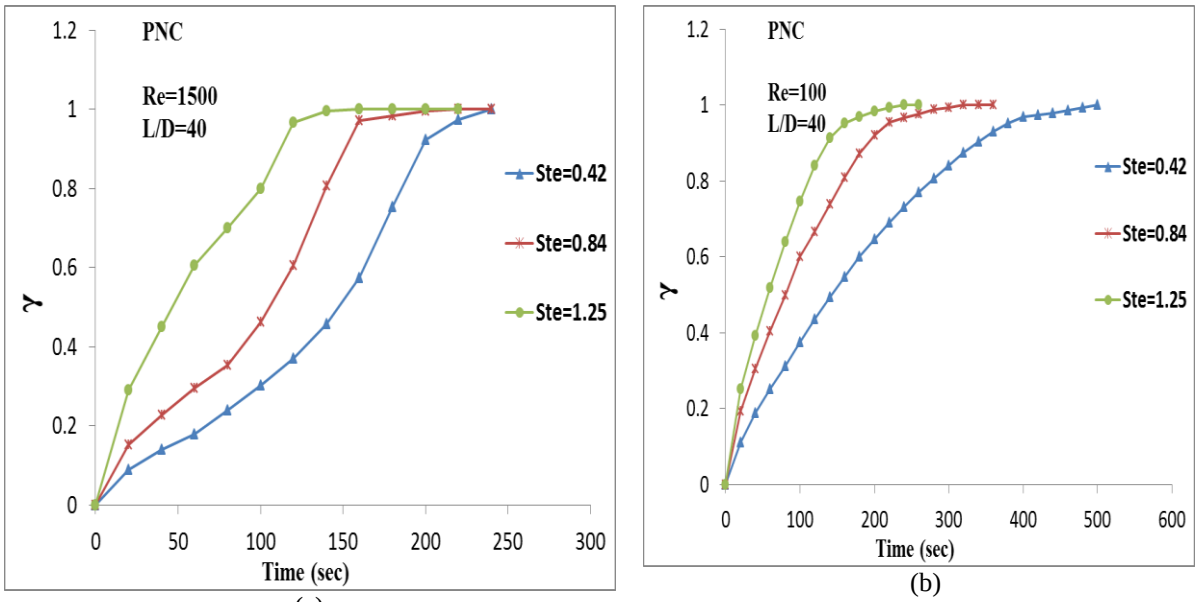

(a) (b)

Figure 7. Impact of Ste number on average liquid fraction: (a) Re=1500, (b) Re=100

As noticed from Figures 6a and 6b, the variation of Ste number has no effect on the local Nu number trends. This is occurred as a result of the Nu number is determined at constant physical properties with the temperature. Alternatively, from Figures 7a and 7b, the higher Ste number accounts to higher melting rate compared to that at low Ste number, this is because the higher Ste number leads to higher natural convection currents and accordingly faster melting rate for high inlet HTF temperature. It is remarkable to observe that the difference in the melting rate for the three different values of Ste numbers at high Re number is more pronounced than that at low Re number. At high Re number, the HTF has high HTC and any increase in the wax HTC will significantly enhance the overall HTC between the HTF and the wax. In contrast, at low Re number the HTC for the HTF is low and any enhancement in the wax thermal resistance causes insignificant improvement in the overall HTC between both fluids. In addition, the full melting time at the three different values of Ste numbers for high Re number is almost the same as observed from Figure 7a. While in Figure 8b, the three different Ste numbers have different full melting time at low Re number. It may be concluded from those Figures that the design with low HTF mass flow rate or slow inlet velocity in the thermal storage system should be pursued by high inlet HTF temperature to accredit fast melting time otherwise the process requires long time to be accomplished. This is considered during the attendance of free convection flow in the PCM.

4.1.3 Effect of Fourier (Fo) number

At a small Re number, there is no influence of changing of Fo number on the thermal behavior of the HTF either in case of presence of natural convection (PNC) or with (ANC) as shown in Figure 8a and 8b. However, at high Re number, there is a notable difference in local Nu number particularly at presence of natural convection case. Instead, the variation in local Nu number is unnoticeable during absence of natural convection in high Re number as shown in Figure 9b. The explanation of that is the wall temperature is computed by the magnitude of thermal resistances of the HTF and PCM. At high Re number, the thermal resistance of HTF is small, the wall temperature tries to be fixed at constant value. As the melting process proceeds at company of free convection, a thermal boundary layer of the wax constitutes and affects negatively the wall heat flux. The net outcome is the dropping in HTC for the HTF as long as the time goes, as shown in Figure 9a. Alternatively, at absence of free convection, the drop in the wall heat flux is not significantly as that at the presence of natural convection, this leads to meaningless impact on the local Nu number at Re= 1500 as presented in Figure 9b. At low Re number, both wall temperature and heat flux decrease by the same rate with the melting time. The net product is the variation in local Number is not considerable either in presence or absence of natural convection at low Re number, as in Figure 8a and 8b.

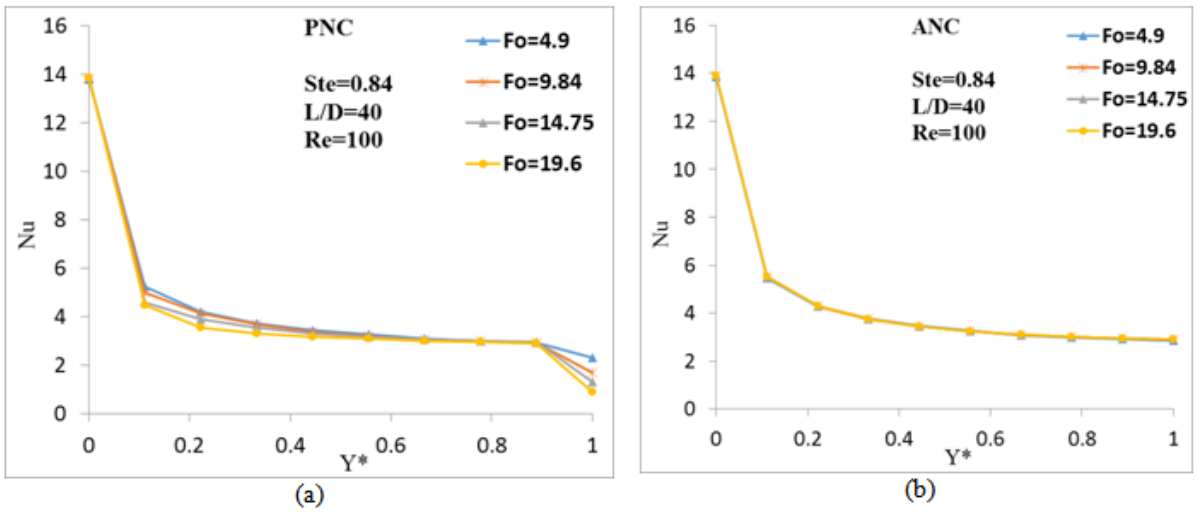

Figure 8. Impact of Fo number on Local Nu number at Re = 100: (a) PNC, (b) ANC

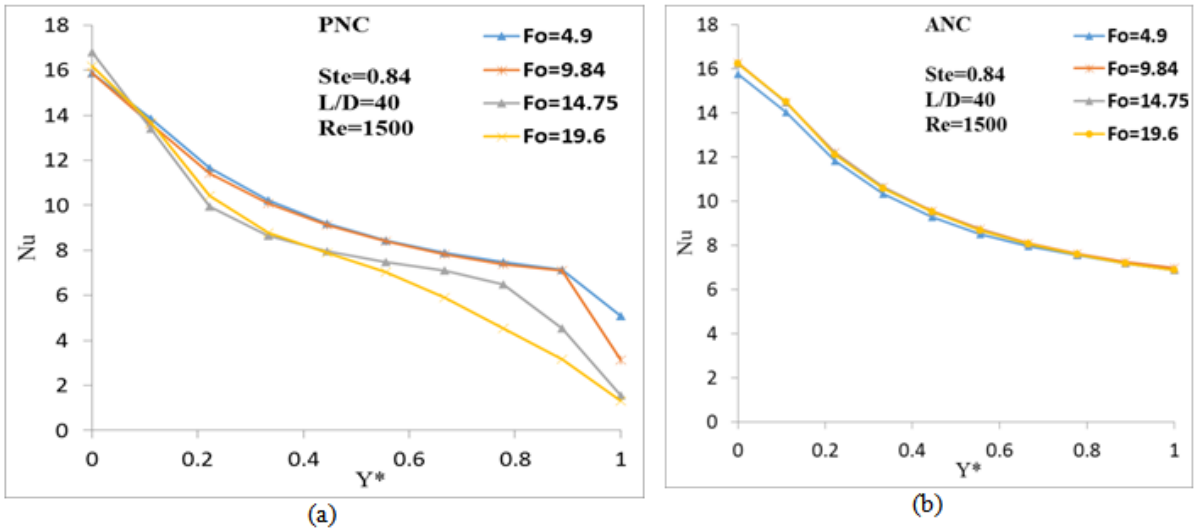

Figure 9. Impact of Fo number on Local Nu number at Re = 1500 : (a) PNC, (b) ANC

4.1.4 Effect of Reynolds (Re) number

As predicted, the increase in the HTF velocity poses an enhancement in the local Nu number as it is depicted in Figure 10a. The higher Re number (higher inlet velocity) is corresponding to higher Nu number, however, this is established at expense of high pumping power of HTF. Moreover as shown in Figure 10b, the augmentation in the HTC of the HTF with increasing the Re number will result in shorting the required time for

melting process. From Figure 10b, at average liquid fraction of 0.7, the time required is 90 seconds at Re=2000, where it is 150 seconds at Re=100 i.e. the decrease in the melting time is 66.7% at expense of increasing the required input driving power of 400%. However, the required input pumping power for the water liquid minichannels is fractions of Walt. Therefore, the miniscaled thermal storage should be designed with high inlet velocity irrespective of the influence of the high entering velocity on the input pumping power. However, for thermal storage of ordinary size, the inlet HTF velocity should be selected prudently provided no severe burden on the input driving power.

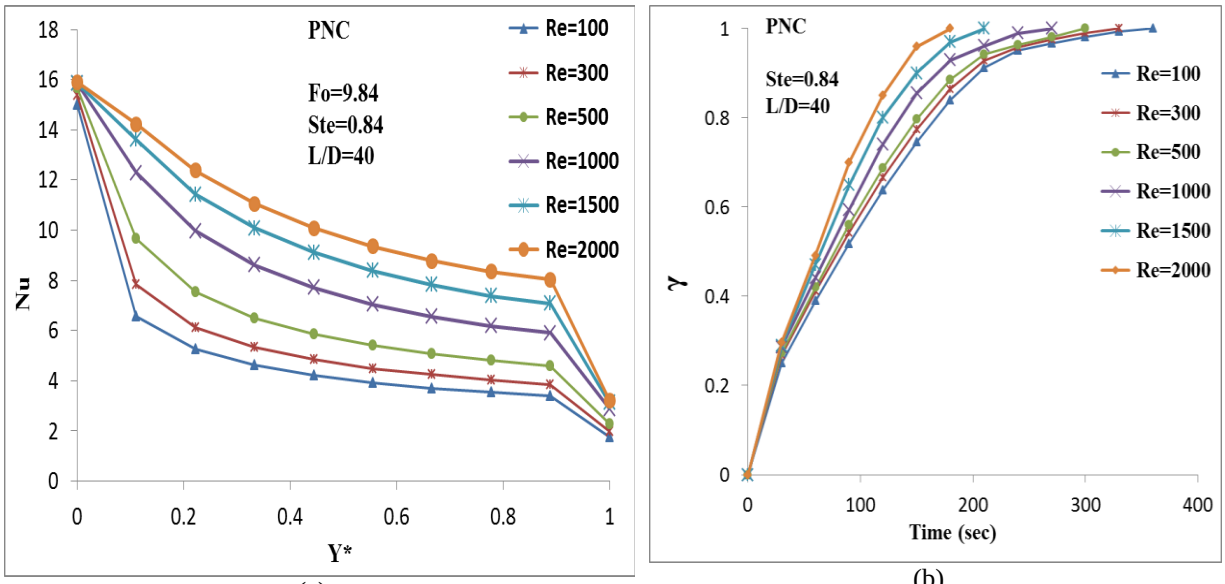

(a) (b)

Figure 10. Impact of Re number on Local Nu number (a) and on average liquid fraction (b)

4.2 Comparison with the traditional constant heat flux (CHF) and constant wall temperature (CWT)

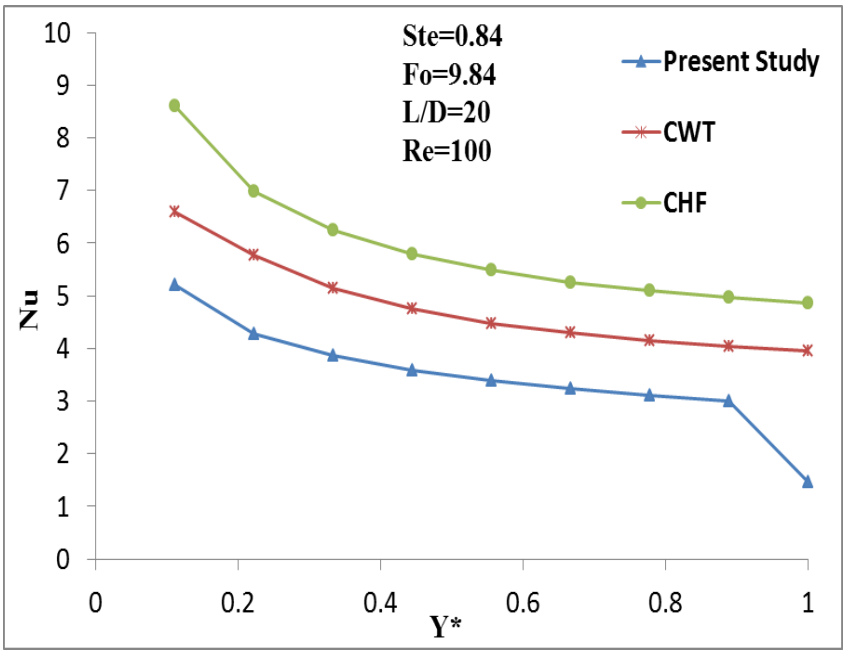

Figure 11. Local Nu number (Present study, CWT, and CHF) along the MC length

As shown in Figure 11, there is an obvious difference between the Local Nu number values along the MC and those obtained at CHF and CWT (they are calculated from [17]) as boundary conditions for the HTF. Hence, the use of traditional correlations (CWT and CHF) can cause substantial errors on designing and analyzing the thermal storage system. For example, from Figure 11, the average Nu number for the present

study is 3; however, it is 5 and 6 for CWT and CHF, respectively, this indicates at least a 66.7 % difference between the present study and the traditional ones. Therefore, development of new correlations for those cases is considered crucial for the designers of those systems. These correlations can be implemented in small and large-scale thermal storage channels.

- **Average Nu number in the PNC case**

The Equation (20) represents the average Nu number during the PNC as a function of the key parameters of the present study.

$$Nu = 10.82 - \frac{38.91}{(4.926 + 0.0033 \times Re)} + \frac{62.83 + 0.6393 \times Re - 0.02485 \times Re \times Fo - 0.3}{5.499 \times \left(\frac{L}{D}\right) + 0.03259 \times Re \times \left(\right.} \quad (20)$$

For: $100 \le \mathrm{Re} \le 2000$ $0.4 \le Ste \le 1.25$ $0 \le Fo \le 20$

- **Average Nu number in the ANC case**

The Equation (21) represents the average Nu number in the ANC as a function of the key parameters of the present study.

$$Nu = 4.748 + 0.01135 \times Re + 9.87e^{-10} \times Re^3 - 4.361e^{-6} \times Re^2 - 0.000106 \times \left(\frac{L}{D}\right)^2 - 2.$$
$$\times \sin\left(0.5262 + 0.944 \times \frac{L}{D}\right) - 0.005503 \times Re \times \sin\left(0.5262 + 0.944 \times \frac{L}{D}\right) \quad (21)$$

For: $100 \le \mathrm{Re} \le 2000$ $0.4 \le Ste \le 1.25$

Table 1 is prepared to verify and test the output of those correlations with those obtained from the numerical model of the present study. The comparison shows that the maximum deviance between both outcomes is of 1.41%. A comparison between the output results (calculation of Nu number) from the new developed correlations with those obtained from traditional ones (CHF and CWT correlations) is given in Table 2. As noticed from this Table that the results obtained from the traditional correlations, deviate from the new developed ones with maximum deviation of -38.89%.

Table 1. Comparsion between the new developed correlations with the present numerical model in terms of calculation of Nu number

Equation	Conditions	Present model (new correlation)	Present model (Numerical)	Deviation (%)
(20)	Re=1000; Fo=9.84; L/D=40	8.18	8.15	**0.37**
(20)	Re=500; Fo=9.84; L/D=10	10.9	11	**-0.91**
(20)	Re=100; Fo=4.9; L/D=100	3.6	3.55	**1.41**
(21)	Re=1000; Fo=9.84; L/D=40	8.5	8.4	**1.19**
(21)	Re=500; Fo=9.84; L/D=10	12	11.9	**0.84**
(21)	Re=100; Fo=4.9; L/D=100	3.7	3.75	**-1.33**

Table 2. Comparsion between the new developed correlations with the traditional correaltions in terms of calculation of Nu number

Equation	Conditions	Present model (new correlation)	CHF	CWT	Maximum Deviation (%)
(20)	Re=1000; Fo=9.84; L/D=40	8.18	11	7	**-34.47**
(20)	Re=500; Fo=9.84; L/D=10	10.9	12.5	8	**-14.68**
(20)	Re=100; Fo=4.9; L/D=100	3.6	5	4	**-38.89**
(21)	Re=1000; Fo=9.84; L/D=40	8.5	11	7	**-29.41**
(21)	Re=500; Fo=9.84; L/D=10	12	12.5	8	**33.33**
(21)	Re=100; Fo=4.9; L/D=100	3.7	5	4	**-35.14**

V. Conclusions

In this work, a mini-channel thermal storage system was studied. Numerical analysis was conducted using ANSYS FLUENT to study the thermal characteristics of the HTF in the melting process during the PNC currents. An experimental test rig was built to validate the numerical results and a decent accordance was achieved with maximum deviation of 5 %. Several parameters (L/D, Ste, Fo, and Re numbers) were taken into consideration to investigate their effect on the thermal characteristics of the HTF and on the melting behavior of the PCM;

The key outcomes from this work can be listed as follows:

a) The change in L/D ratio has no effect on the melting rate at high Re numbers, while at small Re number it has a noticeable effect on the melting rate. The longer channel has the longer melting time at low Re number.
b) The increase in Ste number does not make any change in the local Nu number (constant properties of the HTF), the full melting time is almost the same at any Ste number at high Re number. However, the increase in Ste number poses to a reduction in the full melting time at low Re number. Therefore, it is recommended to have high inlet HTF temperature during low inlet velocity of the fluid.
c) At high Re number, the change in Fo number leads to substantial variation in the local Nu number particularly during the PNC. However, the influence of Fo number on the local Nu number is meaningless at small Re numbers.
d) The key parameter which affects significantly the HTF and the PCM thermal characteristics is the Re number. The increase in the Re number from 100 to 2000 causes an increase in the average Nu number from 5 to 11 and decreases the time required for melting from 350 to 175 seconds.
e) As a comparison to the traditional correlations (CWT and CHF), there is a considerable deviation in the prediction of the Nu number for the HTF during melting of the PCM either for PNC currents or ANC currents. The maximum deviation can reach to 66.7% between the average value of Nu number of the developed correlation and that obtained from traditional correlations.

As a result, the present study developed new correlations that can be used and implemented for melting process during presence/absence of free convection currents to calculate the average Nu number.

Reference

[1]. Martin Longeon, Adèle Soupart, Jean-François Fourmigué, Arnaud Bruch, Philippe Marty: Experimental and numerical study of annular PCM storage in the presence of natural convection. Applied Energy 112 (2013) 175–184.
[2]. Atul Sharma, V.V. Tyagi, C.R. Chen, D. Buddhi: Review on thermal energy storage with phase change materials and applications. Renewable and Sustainable Energy Reviews 13 (2009) 318–345
[3]. M Khamis Mansour: Effect of natural convection on conjugate heat transfer characteristics in liquid mini-channel during phase change material melting. Proc IMechE Part C: Journal of Mechanical Engineering Science 2014, Vol. 228(3) 491–513.
[4]. Brousseau P and Lacroix M. Numerical simulation of a multi-layer latent heat thermal energy storage system. International Journal of Energy Research 1998; 22: 1–15.
[5]. Okada M. Characteristic of a plate-fin heat exchanger with phase change materials. Journal Enhanced Heat Transfer 1995; 2(4): 273–281.
[6]. Majumadr P and Saidbakhsh A. A heat transfer model for phase change thermal energy storage. Heat Recovery System CHP 1990; 10(56): 457–468.
[7]. Farid MM and Husian RM. An electrical storage heater using the phase change method of heat storage. Energy Conversion Management 1990; 30(3): 219–230.
[8]. Smith RN, Ebersole TE and Griffin FP. Heat Exchanger performance in latent heat thermal energy storage. Journal of Solar Energy 1980; 102: 112–118.
[9]. Bellecci C and Conti M. Phase change thermal storage: transient behavior analysis of a solar receiver / storage module using the enthalpy method. International Journal of Heat and Mass Transfer 1993; 36(8): 2157–2163.
[10]. Bellecci C and Conti M. Latent heat thermal storage for solar dynamic power generation. Solar Energy 1993; 51(3): 169–173.
[11]. Bellecci C and Conti M. Transient behaviour analysis of a latent heat thermal storage module. International Journal of Heat and Mass Transfer 1993; 36(15): 3851–3857.
[12]. Hamid El Qarnia. Theoretical study of transient response of a rectangular latent heat thermal energy storage system with conjugate forced convection. Energy Conversion Management 2004; 45: 1537–1551.
[13]. Trp A. A numerical and experimental study of transient heat transfer in a shell-and-tube latent heat storage unit with paraffin as a phase change material. Energy Environ 2002; vol. II: 35–46.
[14]. Erek A. Phase change around a finned tube. Journal Engineering Science 2002; 9: 15–21.
[15]. Kota K, Chow L and Leland Q. Laminar film condensation driven latent thermal energy storage in rectangular containers. International Journal of Heat and Mass Transfer 2012; 55: 1208–1217.
[16]. Zhang Y and Faghri A. Semi-analytical solution of thermal energy storage system with conjugate laminar forced convection. International Journal of Heat and Mass Transfer 1996; 39: 717–724. .
[17]. R. Shankar Subramanian: Heat Transfer in Flow through Conduits. Department of Chemical and Bio-molecular Engineering, Clarkson University.